Chapter 9
Comments on Tetrahedron-Type Equation for Non-crystallographic Coxeter Groups

Abstract This short chapter is a supplement recalling some basic facts on non-crystallographic finite Coxeter groups and raising questions concerning a possible tetrahedron-type equation.

9.1 Finite Coxeter Groups

The list of finite Coxeter groups[1] is given by [59]:

$$\begin{aligned} &A_n\,(n\geq 1),\ B_n\,(n\geq 2),\ D_n\,(n\geq 4),\ E_6,\ E_7,\ E_8,\ F_4,\ G_2,\\ &H_2,\ H_3,\ H_4,\ I_2(m)\,(m\geq 3). \end{aligned} \tag{9.1}$$

The indices are called ranks. The alphabetically last one $I_2(m)$ is the dihedral group which is the order $2m$ group of symmetry of a regular m-gon consisting of orthogonal transformations. It has overlap with the other rank 2 members for $m = 3, 4, 6$. See Fig. 9.2. Rank n Coxeter groups have a presentation in terms of generators $s_1, \dots, s_n$ obeying the relations $(s_i s_j)^{m_{ij}} = 1$ with $m_{ii} = 1$ and $m_{ij} = m_{ji} \in \{2, 3, \dots\} \cup \{\infty\}$ for $i \neq j$, where $m_{ij} = \infty$ is to be understood as no relation. The data $\{m_{ij}\}$ is customarily encoded in the Coxeter graph. Its vertex set is $\{1, 2, \dots, n\}$, and the two vertices i and j are connected by an unlabeled edge if $m_{ij} = 3$ and by an edge labeled with m_{ij} if $4 \leq m_{ij} < \infty$. The case $\forall m_{ij} \in \{2, 3, 4, 6\}$ is called crystallographic, and has a realization as the Weyl group of the corresponding Lie algebras. Thus those on the second line in (9.1), except $m = 3, 4, 6$, are the non-crystallographic finite Coxeter groups (Fig. 9.1).

[1] In this chapter, symbols like A_n are used to mean Coxeter groups instead of Lie algebras, unlike elsewhere in the book.

A. Kuniba, *Quantum Groups in Three-Dimensional Integrability*, Theoretical and Mathematical Physics, https://doi.org/10.1007/978-981-19-3262-5_9

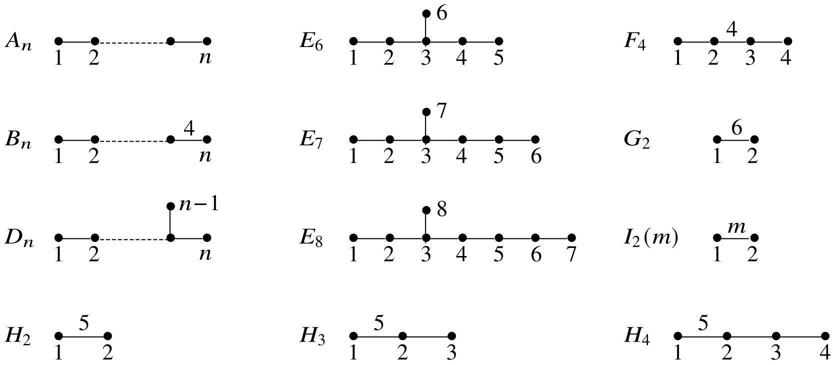

Fig. 9.1 Coxeter graphs of (9.1). Unlike the Dynkin diagrams, there is no arrow and C_n has been merged into B_n

The dihedral groups $I_2(m)$ and H_2, H_3, H_4 admit various embeddings as shown in Fig. 9.2.

Fig. 9.2 Various embeddings concerning non-crystallographic Coxeter groups

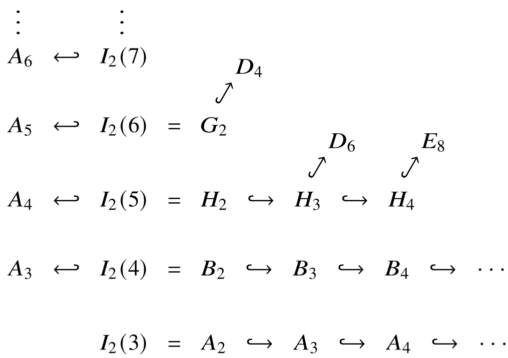

The embedding of type $X_n \hookrightarrow X_{n+1}$ just means that X_n is a parabolic subgroup of X_{n+1}. Denoting the generators in the image by t_i's, the other cases are given as follows [134]:

$$I_2(m) \hookrightarrow A_{m-1} : s_1 \mapsto \prod_{\substack{1 \le j \le m-1 \\ j:\text{odd}}} t_j, \quad s_2 \mapsto \prod_{\substack{1 \le j \le m-1 \\ j:\text{even}}} t_j, \tag{9.2}$$

$$G_2 \hookrightarrow D_4 : s_1 \mapsto t_1 t_3 t_4, \quad s_2 \mapsto t_2, \tag{9.3}$$

$$H_3 \hookrightarrow D_6 : s_1 \mapsto t_3 t_5, \quad s_2 \mapsto t_2 t_4, \quad s_3 \mapsto t_1 t_6, \tag{9.4}$$

$$H_4 \hookrightarrow E_8 : s_1 \mapsto t_4 t_8, \quad s_2 \mapsto t_3 t_5, \quad s_3 \mapsto t_2 t_6, \quad s_4 \mapsto t_1 t_7. \tag{9.5}$$

The embedding $B_2 \hookrightarrow A_3$ is a folding by the order 2 diagram automorphism, and has the generalization to $B_n \hookrightarrow A_{2n-1}$ $(n \geq 2)$ as $s_i \mapsto t_i t_{2n-i}$ $(1 \leq i < n)$ and $s_n \mapsto t_n$.

9.2 Tetrahedron-Type Equation for the Coxeter Group H_3

For any element w of a Coxeter group, one can consider a reduced expression (rex) graph. The vertices are reduced expressions of w and the two are connected by an edge if and only if they are transformed by a single application of the Coxeter relation $(s_i s_j)^{m_{ij}} = 1$ $(i \neq j)$. According to [126, Theorem 2.17], any non-trivial loop in a rex graph is generated from the loops in the rex graph of the longest element in the parabolic subgroups of rank 3. See also [44, Sect. 1.4.3]. In this sense, rank 3 cases are essential. In fact, we have seen that the A_3 and B_3 cases led to the tetrahedron and the 3D reflection equations[2] in earlier chapters, respectively. The remaining case is H_3, which we shall consider in what follows.

The Coxeter group H_3 is known as the symmetry of the icosahedron or equivalently the dual dodecahedron [59]. The relations of the generators s_1, s_2, s_3 read as $s_1^2 = s_2^2 = s_3^2 = 1$ and

$$s_1 s_3 = s_3 s_1, \quad s_2 s_3 s_2 = s_3 s_2 s_3, \quad s_1 s_2 s_1 s_2 s_1 = s_2 s_1 s_2 s_1 s_2. \tag{9.6}$$

Unlike the case of crystallographic Coxeter groups, the approach by a quantized coordinate ring is not available. However, one can formulate a compatibility equation formally by an argument similar to those for the crystallographic cases. We attach operators to the transformations in (9.6), denoted by only indices, as follows:

$$P = P^{-1} : 13 \to 31,\ 31 \to 13, \tag{9.7}$$

$$\Phi : 232 \to 323, \quad \Phi_{ijk} = R_{ijk} P_{ik}, \tag{9.8}$$

$$\Omega : 21212 \to 12121, \quad \Omega_{ijklm} = Y_{ijklm} P_{im} P_{jl}, \tag{9.9}$$

where, as before, the lower indices $i, j, k, \ldots$ of the operators specify the components that they act on non-trivially. The operators Ω and Y are the characteristic ones which are expected to come from H_2.

A reduced expression of the longest element of H_3 is

$$s_1 s_2 s_1 s_2 s_1 s_3 s_2 s_1 s_2 s_1 s_3 s_2 s_1 s_2 s_3, \tag{9.10}$$

which has the length 15. Now the process analogous to (3.93), (5.106) and (7.16) reads as

[2] We have actually encountered a fine difference between B_3 and C_3 versions originating in the relevant quantized coordinate rings.

$$
\begin{array}{ll}
1212\underline{13}212132123 & P_{5,6} \\
12123\underline{12121}32123 & \Omega^{-1}_{6,7,8,9,10} \\
121\underline{232}121\underline{232}123 & \Phi_{4,5,6}\Phi_{10,11,12} \\
12\underline{13}2\underline{31}21\underline{13}2\underline{31}23 & P_{3,4}P_{6,7}P_{9,10}P_{12,13} \\
123121\underline{323}121\underline{323} & \Phi^{-1}_{7,8,9}\Phi^{-1}_{13,14,15} \\
12312123\underline{21212}32 & \Omega_{9,10,11,12,13} \\
1231212\underline{31}212\underline{13}2 & P_{8,9}P_{13,14} \\
123\underline{12121}3212312 & \Omega^{-1}_{4,5,6,7,8} \\
1\underline{232}121\underline{232}12312 & \Phi_{2,3,4}\Phi_{8,9,10} \\
132\underline{31}2\underline{13}2\underline{31}2312 & P_{4,5}P_{7,8}P_{10,11} \\
\underline{13}21\underline{323}121\underline{323}12 & P_{12}\Phi^{-1}_{567}\Phi^{-1}_{11,12,13} \\
312123\underline{21212}3212 & \Omega^{-1}_{7,8,9,10,11} \\
31212\underline{31}212\underline{13}212 & P_{6,7}P_{11,12} \\
3\underline{12121}321231212 & \Omega^{-1}_{2,3,4,5,6} \\
32121\underline{232}1231212 & \Phi_{6,7,8} \\
3212\underline{13}2\underline{31}231212 & P_{5,6}P_{8,9} \\
32123121\underline{323}1212 & \Phi^{-1}_{9,10,11} \\
3212312123\underline{21212} & \Omega_{11,12,13,14,15} \\
321231212312121. &
\end{array}
\tag{9.11}
$$

It reverses the initial reduced word. There is another route achieving the reverse ordering which is related to (9.11), similarly to (7.17) and (7.18). Equating the two ways, substituting (9.7), (9.9) and assuming that $P_{i,j}$ just exchanges the indices as $P_{4,7}Y_{1,3,4,9} = Y_{1,3,7,9}P_{4,7}$ etc., we get the H_3 analogue of the tetrahedron equation:

$$
\begin{aligned}
& Y_{11,12,13,14,15}R^{-1}_{15,10,9}R_{5,7,15}Y^{-1}_{15,6,4,3,2}Y_{2,5,8,10,14}R^{-1}_{14,7,3}R^{-1}_{13,9,2}R_{1,6,14} \\
& \times R_{3,8,13}Y^{-1}_{13,10,7,4,1}Y_{1,3,5,9,12}R^{-1}_{12,8,4}R^{-1}_{11,2,1}R_{6,10,12}R_{4,5,11}Y^{-1}_{11,9,8,7,6} \\
& = Y_{6,7,8,9,11}R^{-1}_{11,5,4}R^{-1}_{12,10,6}R_{1,2,11}R_{4,8,12}Y^{-1}_{12,9,5,3,1}Y_{1,4,7,10,13}R^{-1}_{13,8,3} \\
& \times R^{-1}_{14,6,1}R_{2,9,13}R_{3,7,14}Y^{-1}_{14,10,8,5,2}Y_{2,3,4,6,15}R^{-1}_{15,7,5}R_{9,10,15}Y^{-1}_{15,14,13,12,11}.
\end{aligned}
\tag{9.12}
$$

There are 6 $Y^{\pm1}$'s and 10 $R^{\pm1}$'s on each side. If $Y^{-1}_{ijklm} = Y_{ijklm} = Y_{mlkji}$ and $R^{-1}_{ijk} = R_{ijk} = R_{kji}$ are valid, the above equation reduces to

$$
\begin{aligned}
& Y_{11,12,13,14,15}R_{9,10,15}R_{5,7,15}Y_{2,3,4,6,15}Y_{2,5,8,10,14}R_{3,7,14}R_{2,9,13}R_{1,6,14} \\
& \times R_{3,8,13}Y_{1,4,7,10,13}Y_{1,3,5,9,12}R_{4,8,12}R_{1,2,11}R_{6,10,12}R_{4,5,11}Y_{6,7,8,9,11} \\
& = \text{product in reverse order.}
\end{aligned}
\tag{9.13}
$$

A diagrammatic representation of the reduced version (9.13) of the H_3 compatibility equation is available in [44, Eq. (4.9)].

9.3 Discussion on the Quintic Coxeter Relation

The operator Y has been introduced formally in (9.9) in association with the quintic Coxeter relation. It is natural to seek it in the parabolic subgroup $H_2 \subset H_3$. In this section, we study a composition of the birational 3D R (Sect. 3.6.2) corresponding to the transformation of $s_1s_2s_1s_2s_1$ into $s_2s_1s_2s_1s_2$ in H_2 under the embedding $H_2 \hookrightarrow A_4$.

The embedding is the $m = 5$ case of (9.2), which reads as $s_1 \mapsto t_1t_3$, $s_2 \mapsto t_2t_4$. One way to realize $s_1s_2s_1s_2s_1 = s_2s_1s_2s_1s_2$ in the image is the following transformation of the reduced expression of the longest element of A_4:

$$
\begin{array}{ll}
\underline{13}2\underline{41}32\underline{41}3 & P_{1,2}P_{4,5}P_{8,9} \\
3\underline{121}432143 & \Phi_{2,3,4} \\
321\underline{24}32143 & P_{4,5} \\
3214\underline{232}143 & \Phi_{5,6,7} \\
321432\underline{31}43 & P_{7,8} \\
3214321\underline{343} & \Phi_{8,9,10} \\
32143\underline{214}34 & P_{6,7}P_{7,8} \\
321\underline{434}2134 & \Phi_{4,5,6} \\
32\underline{13}432134 & P_{3,4} \\
\underline{323}1432134 & \Phi_{1,2,3} \\
2321432\underline{13}4 & P_{8,9} \\
23214\underline{323}14 & \Phi_{6,7,8} \\
2321\underline{42}3214 & P_{5,6} \\
23\underline{212}43214 & \Phi_{3,4,5} \\
2312\underline{143}214 & P_{6,7}P_{5,6} \\
231\underline{24}3\underline{121}4 & P_{4,5}\Phi_{7,8,9} \\
2314\underline{232}124 & \Phi_{5,6,7} \\
2\underline{31}432\underline{31}24 & P_{7,8}P_{2,3} \\
21\underline{343}21324 & \Phi_{3,4,5} \\
2\underline{14}3\underline{42}1324 & P_{2,3}P_{5,6} \\
2413241324. &
\end{array} \tag{9.14}
$$

As before, we have assigned an operator to each step, where P_{ij} is the transposition and $\Phi_{ijk} = R_{ijk}P_{ik}$ with $R_{ijk} = R^{\lambda}_{ijk}$ being the λ-deformed biraitonal 3D R (3.159).[3] The composition of the operators in (9.14) is rearranged as $\tilde{Y}\sigma$, where σ is a product of P_{ij}'s giving the reverse ordering permutation in $\mathfrak{S}_{10}$, and $\tilde{Y}$ has the form

$$\tilde{Y} = R_{2,4,6}R_{2,5,8}R_{2,7,9}R_{3,8,9}R_{3,5,7}R_{1,6,9}R_{1,4,7}R_{1,3,10}R_{4,5,10}R_{6,8,10}. \tag{9.15}$$

This is a totally positive involutive rational map of 10 variables $(x_1, \dots, x_{10})$. Set $(x'_1, \dots, x'_{10}) = \tilde{Y}((x_1, \dots, x_{10}))$. Then examples of simplest components are

$$x'_2 = \frac{x_2x_4x_5x_7}{x_2x_4x_5 + x_2x_4x_9 + x_2x_8x_9 + x_6x_8x_9 + \lambda x_2x_4x_9(x_5x_7 + x_5x_8 + x_6x_8)}, \tag{9.16}$$

$$x'_{10} = x'_2|_{x_1\leftrightarrow x_9, x_2\leftrightarrow x_{10}, x_3\leftrightarrow x_7, x_4\leftrightarrow x_8}. \tag{9.17}$$

One can directly check:

Proposition 9.1 *The map $\tilde{Y}$ preserves the following:*

$$x_2x_4x_5x_7, \quad x_3x_5x_8x_{10}, \quad x_1x_3x_4x_5x_6x_8, \quad x_4x_5x_6x_7x_8x_9, \tag{9.18}$$

$$\{(x_1, \dots, x_{10}) \mid x_7 = x_3, x_8 = x_4, x_9 = x_1, x_{10} = x_2\}. \tag{9.19}$$

One can get totally positive involutive maps of 5 variables by restricting the 6-dimensional space (9.19) by a conserved quantity. For instance, imposing $a = x_2x_4x_5x_7$ in the space (9.19) leads to the map $(x_1, x_2, x_3, x_4, x_6) \mapsto (x''_1, x''_2, x''_3, x''_4, x''_6)$ defined by

$$\begin{aligned}&(x''_1, x''_2, x''_3, x''_4, \frac{a}{x''_2x''_3x''_4}, x''_6, x''_3, x''_4, x''_1, x''_2)\\ &= \tilde{Y}((x_1, x_2, x_3, x_4, \frac{a}{x_2x_3x_4}, x_6, x_3, x_4, x_1, x_2))\end{aligned} \tag{9.20}$$

depending on the parameter a. However, there is no canonical way of doing such a reduction, and construction of a solution to the H_3 compatibility equation (9.12) or (9.13) remains as a challenge.

These features, especially the discrepancy of (9.19) from the desired dimension 5, stem from the fact that H_2 viewed as a subgroup A_4 is *not* an invariant of the diagram automorphism. In contrast, for the embedding $B_2 \hookrightarrow A_3$ respecting the diagram automorphism, the composition of the birational 3D R's corresponding to the length 6 longest element of A_3 admits a natural restriction to the 4-dimensional subspace

[3] $\Phi^{-1} = \Phi$ has been taken into account due to $P^{-1} = P$, $R^{-1} = R$, $R_{ijk} = R_{kji}$.

matching the 3D K [152] and reproduces [110, Remark 5.1]. Another example of such an embedding is $G_2 \hookrightarrow D_4$, which allows one to construct a λ-deformation of the birational 3D F (8.74).[4]

[4] Private communication with the author of [152].